

METHODOLOGY

Open Access



CRISPR-mediated generation and comprehensive phenotyping of Duchenne Muscular Dystrophy mouse models

Jayshen Arudkumar^{1,2}, Yu C. J. Chey^{1,2}, Sandra G. Piltz^{1,2,3}, Paul Q. Thomas^{1,2,3*} and Fatwa Adikusuma^{1,2*}

Abstract

Background Duchenne Muscular Dystrophy (DMD) is a severe, progressive muscle-wasting disorder predominantly affecting boys, with an incidence of 1 in 5,000 births. It is caused by loss-of-function mutations in the X-linked *DMD* gene, which encodes the dystrophin protein essential for muscle integrity. CRISPR-Cas9 gene-editing technology has enabled precise and permanent modifications to DNA, facilitating the generation of diverse animal models for studying genetic disorders such as DMD. This study aims to establish a protocol for generating mouse models of DMD using CRISPR-Cas9, alongside comprehensive guidelines for their phenotypic and molecular characterisation, to support researchers investigating potential treatments for DMD.

Methods We employed CRISPR-Cas9 microinjection of mouse embryos to produce murine models with exon-51 and exon-52 deletions, mimicking common DMD mutations seen in patients. The DMD models were validated through DNA, RNA, and protein analyses. The protocol also includes functional assessments such as forelimb grip strength testing, histological examination, and serum creatine kinase (CK) testing to evaluate muscle damage and dystrophic pathology.

Results Generation of murine models with DMD-associated mutations was confirmed through molecular analysis, including Western blot and immunostaining, which revealed the absence of dystrophin. Functional assays demonstrated hallmark DMD characteristics, such as reduced muscle strength and elevated CK levels. Histological analysis of muscle tissue consistently showed dystrophic features, including centrally nucleated myofibers, fibrotic deposition, and variability in myofiber size, all consistent with DMD pathology. These findings confirm the utility of our DMD mouse models in replicating disease traits.

Discussion This comprehensive protocol provides a standardised and accessible framework for generating and characterising DMD mouse models, addressing the need for cohesive methodologies. Our approach enables in-depth investigation of DMD pathophysiology and offers a reliable platform for testing therapeutic strategies. By establishing these protocols, we aim to accelerate DMD research and therapeutic development, with applications extending to the study of other genetic disorders.

Keywords CRISPR-Cas9, DMD, BMD, Therapy, Dystrophy, Phenotyping, Mouse model, Musculoskeletal

*Correspondence:

Paul Q. Thomas

paul.thomas@adelaide.edu.au

Fatwa Adikusuma

fatwa.adikusuma@adelaide.edu.au

Full list of author information is available at the end of the article



© The Author(s) 2024. **Open Access** This article is licensed under a Creative Commons Attribution-NonCommercial-NoDerivatives 4.0 International License, which permits any non-commercial use, sharing, distribution and reproduction in any medium or format, as long as you give appropriate credit to the original author(s) and the source, provide a link to the Creative Commons licence, and indicate if you modified the licensed material. You do not have permission under this licence to share adapted material derived from this article or parts of it. The images or other third party material in this article are included in the article's Creative Commons licence, unless indicated otherwise in a credit line to the material. If material is not included in the article's Creative Commons licence and your intended use is not permitted by statutory regulation or exceeds the permitted use, you will need to obtain permission directly from the copyright holder. To view a copy of this licence, visit <http://creativecommons.org/licenses/by-nc-nd/4.0/>.

Introduction

Duchenne Muscular Dystrophy (DMD) is a progressive and fatal muscle-wasting disorder, primarily affecting boys, with an estimated incidence of 1 in 5,000 births. There are a wide range of causative loss-of-function mutations in the X-linked *DMD* gene that encodes for the dystrophin protein [1, 2]. The most prevalent are large deletions, of which 80% occur within mutational hot-spots within exons 2–20 and 45–55 [3]. The absence of muscle dystrophin protein results in muscle wasting and damage, leading to the loss of independent ambulation during the pre-teen years. This condition becomes more severe with age, resulting in premature mortality due to progressive wasting of respiratory muscles and development of dilated cardiomyopathy [4]. Several therapies have been developed to combat this disorder, although they are transient in effect with limited functional benefit on patients. As such, there remains no curative treatment option present for DMD [4].

The CRISPR-Cas9 gene editing technology utilises single guide RNA (sgRNA) coupled with Cas9 endonuclease to generate precise double-stranded breaks (DSBs) at targeted DNA sequences [5]. These breaks prompt the cell's innate DNA damage repair mechanisms, predominantly the error-prone non-homologous end joining (NHEJ) pathway active throughout the cell cycle, often resulting in insertions or deletions (InDels) surrounding the break site [6]. In instances where two gRNAs are positioned closely on the same chromosome, targeted removal of the intervening region can occur. CRISPR-Cas9 technology signifies a groundbreaking advancement in generating genetically modified animal models [7]. This innovative approach provides a swift and cost-effective method to engineer genetic modifications for animal model creation. Over the past decade, CRISPR-Cas9 has gained global traction in laboratories, transforming the landscape of genetically modified animal model generation with unparalleled speed and precision [7, 8].

The use of CRISPR-Cas9 technology has been instrumental in creating bespoke mouse models for DMD, serving as indispensable tools to explore both the molecular intricacies and physical traits of this condition [8]. These models offer significant insights into disease mechanisms and provide physiologically-relevant platforms for therapeutic development. Moreover, CRISPR-Cas9 has emerged as a potential therapeutic approach for DMD, with numerous studies focusing on developing CRISPR therapies for this condition. Therefore, establishing robust, reliable, and easily accessible protocols for generating DMD mouse models and assessing DMD phenotypes would be beneficial. This could address the current issue of fragmented protocols scattered across multiple publications, thereby simplifying the workflow

for researchers. In this comprehensive protocol, we delineate the step-by-step process for generating DMD mouse models. Specifically, our focus was on creating exon-51 deletion ($\Delta 51$) and exon-52 deletion ($\Delta 52$) mouse models, which are prevalent frameshift-inducing mutations in DMD patients. Our protocol also offers a streamlined, detailed procedure for the thorough physical and molecular characterisation of dystrophic pathology within these models. By following these precise protocols, researchers can conduct meticulous examinations, establishing a robust foundation for further investigations into disease mechanisms and potential therapeutic interventions.

Methods

The protocols described in this article are published on protocols.io (see links below) and are included for printing as supporting information file 1 with this article, updated on 29 January 2024.

There are 9 separate protocols with each of the reserved DOIs listed here:

IVT protocol <https://doi.org/10.17504/protocols.io.36wgq3kdylk5/v1>

Tail Vein Bleeding protocol <https://doi.org/10.17504/protocols.io.dm6gp3kr8vzp/v1>

Post-mortem Tissue protocol <https://doi.org/10.17504/protocols.io.36wgq3z53lk5/v1>

DNA Extraction protocol: <https://doi.org/10.17504/protocols.io.ewov1qw6ygr2/v1>

IF protocol <https://doi.org/10.17504/protocols.io.kqdg3xo5qg25/v1>

H&E protocol <https://doi.org/10.17504/protocols.io.ewov1qw82gr2/v1>

RNA Extraction protocol <https://doi.org/10.17504/protocols.io.36wgq3z3olk5/v1>

Western Blot protocol <https://doi.org/10.17504/protocols.io.x54v9pnpz3e/v1>

Grip strength testing protocol <https://doi.org/10.17504/protocols.io.eq2lyjrjqlx9/v1>

Generation of DMD mouse models

All experiments involving animal use were approved by the South Australian Health & Medical Research Institute (SAHMRI) Animal Ethics Committee. The mice used in this study were housed in the SAHMRI animal facility, under controlled conditions with food and water provided ad libitum. At the experimental endpoint, mice were euthanised using CO₂ asphyxiation followed by cervical dislocation in accordance with approved protocols. No anaesthetics were used prior to euthanasia.

To produce the guide RNAs, we first employed in-silico screening for the selection of intron-targeting guides using CRISPOR [9]. Oligonucleotide pairs containing the gRNA spacer sequences were cloned into the pSpCas9(BB)-2A-Puro (PX459) V2.0 (Addgene #62,988) vector [10] using *BbsI*-mediated Golden-Gate cloning method. These vectors were then PCR amplified to produce in vitro transcription (IVT) templates. PCR was performed using the primers listed in S1 Table. In brief, the forward primer contained both T7 promoter and gRNA sequences, while the reverse primer contained the tracrRNA sequence. The PCR amplicon was purified using the QIAquick PCR Purification Kit (Qiagen). The purified PCR products were in-vitro transcribed using the HiScribe T7 Quick High Yield RNA Synthesis Kit (NEB). SpCas9 nuclease mRNA was produced by IVT of Xho-linearised CMV/T7-hCas9 (Toolgen). SpCas9 nuclease mRNA and gRNA were purified using RNeasy Mini Kit (Qiagen). To generate the mouse models, SpCas9 nuclease mRNA (100 ng/ μ l) and two gRNAs (each at 50 ng/ μ l) were injected into the cytoplasm of C57BL/6 J zygotes using a FemtoJet microinjector [11]. Surviving zygotes were transferred into pseudo-pregnant females. Founder males and females with the desired hemizygous knockout and homozygous knockout genotype were then set up for breeding.

Genomic DNA extraction and PCR

Mouse genomic DNA was extracted from the ear notch tissues using the High Pure PCR Template Preparation Kit (Roche), according to the manufacturer's protocol. PCR reactions were set up with Phusion DNA Polymerase (New England Biolabs). PCR primers used in this study can be found in S2 Table.

RNA, cDNA generation, RT PCR and qPCR

Total RNA was extracted from mouse tissues using Trizol reagent (Invitrogen) followed by the RNeasy mini extraction kit (Qiagen). RNA was quantitated using the Nanodrop One Microvolume Spectrophotometer (ThermoFisher Scientific). For cDNA generation, 1–2 μ g of total RNA was used as template for first-strand cDNA synthesis using the High-Capacity cDNA Reverse Transcription Kit (Applied Biosystems) as per the manufacturer's instructions. For SYBR Green RT-qPCR, expression levels of genes were determined using primers spanning the exon-exon boundaries. All 15 μ l RT-qPCR reactions contained 1 μ l cDNA, 1 \times Fast SYBR Green Real-Time PCR master mix (Applied Biosystems) and 0.5 μ M forward and reverse primer mix. Actin Beta (*Actb*) was used as a housekeeping gene to normalise data. Data

was collected and analysed using the QuantStudio Real-Time PCR software (Applied Biosystems).

Dystrophin western blot analysis

For Western blot of skeletal or heart muscle, tissues were homogenised in disruption buffer (15% SDS, 75 mM Tris HCl pH 6.8) and protease inhibitor cocktail (Roche), using green magna lyser tubes (Roche) at 3968 RCF for 2 cycles of 20 s. Samples were then centrifuged at 4 °C at 16,100 RCF for 10 min before isolating the supernatant. Protein concentration was determined by a BCA Protein Assay Kit (ThermoFisher Scientific), and 50 μ g of total protein was loaded onto a NuPAGE™ 3 to 8% Tris-Acetate protein gel (ThermoFisher Scientific). Gels were run at 100 V for 15 min, followed by 120 V for 1 h and 45 min. This was followed by a 10-min transfer using the 'HIGH MW' program in the Trans-Blot Turbo Transfer System (Bio-Rad). The blot was blocked using a 10% Skim milk-PBST for 1 h and then incubated with mouse anti-dystrophin antibody (MANDYS8, Sigma-Aldrich, D8168) at 4 °C overnight [12, 13]. The blot was washed and incubated with goat anti-mouse antibody conjugated with horseradish peroxidase (HRP) (Bio-Rad Laboratories) at room temperature for 1 h. The blot was developed using Super-signal West Femto kit (ThermoFisher Scientific). The loading control was determined by blotting with mouse anti-vinculin antibody (Sigma-Aldrich, V9131).

Histological analysis of muscles

Skeletal muscles from wild-type (WT) and DMD mice were individually dissected and cryo-embedded in 10% Gum Tragacanth (Sigma-Aldrich) on small cork blocks. All embeds were snap frozen in isopentane supercooled in liquid nitrogen. The resulting blocks were stored at –80 °C prior to sectioning. 10 μ m transverse sections of the skeletal muscle and frontal sections of the heart were prepared and air-dried prior to staining. H&E staining was performed with some modifications to the established TREAT-NMD standard operating procedure DMD_M.1.2.007 and a separate study by the Yokota lab [14]. Dystrophin immunohistochemistry was performed using MANDYS8 monoclonal antibody (Sigma-Aldrich) with modifications to the manufacturer's instructions. In brief, cryostat sections were thawed and washed with 4% PFA before being immersed in permeabilisation solution for 10-min. Next, slides were treated with blocking solution and incubated with 1 \times Mouse-on-Mouse IgG Blocking Solution (ThermoFisher Scientific). Slides were then washed and treated with MANDYS8 diluted 1:100 in blocking solution. Following overnight primary antibody incubation at 4 °C, sections were washed, incubated with Donkey anti-Mouse IgG (H+L) Alexa Fluor™ 594,

washed, and nuclei were counterstained with ProLong™ Gold Antifade Mountant with DAPI (ThermoFisher Scientific) prior to coverslipping.

Tail vein bleeding, serum CK and grip strength analysis

Blood was isolated from the tail vein of male mice at P32. A skin numbing cream (EMLA) was applied to the tail of mice, followed by warming the animal in a mini thermacage (Datesand) at 37 °C for 10 min. An incision was made over the lateral vein area of mice under restraint, and blood was collected into a microvette tube. The collected blood samples were allowed to clot at room temperature for 30 min before being spun down at 2000 RCF for 10 min at 4 °C. The resulting colourless serum was frozen at -80 °C for subsequent analysis. Serum creatine kinase levels were measured by a third-party laboratory (Gribbles Veterinary Pathology, Australia), using the ADVIA® Chemistry Creatine Kinase (CK_L) reagent with the ADVIA Chemistry 1800 System. The output values were presented as U/L. For forelimb grip strength testing, each mouse was weighed prior to the test. A force transducer (ANDILOG) equipped with a grasping grid (SDR Scientific) was set up to measure the peak force from each mouse applied during a pull. Pulling the mouse away from the grid once their front paws have clasped onto it revealed the highest force applied. Each mouse performed three series of pulls across four sets for a total of 12 pulls. Each set of three pulls was followed by a resting period of at least one minute. The maximum grip strength was determined by averaging the three highest values and normalising for body weight. The protocol listed here was adapted from the TREAT-NMD standard operating procedure SOP DMD_M.2.2.001 for grip strength testing.

Statistics

All data are presented as mean ± SEM. One-way ANOVA with Tukey's multiple comparisons were performed for comparison between the respective two groups (WT and ΔEx51 DMD mice, WT and ΔEx52 DMD mice). Data analyses were performed with statistical software (GraphPad Prism 10 Software, San Diego, CA, USA). *P* values less than 0.05 were considered statistically significant. Sample sizes for each experiment are stated in the figure legends and represent independent biological replicates in most instances.

General notes and troubleshooting

Conducting the procedures and analyses outlined in this protocol entails several challenges and potential pitfalls (Table 1). One challenge is the difficulty in obtaining mouse founders with the desired deletion. This may arise due to ineffective Cas9-gRNA cutting, often caused

by low-quality Cas9 mRNA or gRNAs used for zygote microinjection. To address these issues, we recommend producing a new batch of Cas9 mRNA or gRNAs. Alternatively, Cas9 mRNA can be obtained from a reputable supplier, or commercial Cas9 protein can be utilised. Additionally, reviewing guide RNA designs and sequences of purchased oligos can help ensure accurate design and oligo quality. Consideration should also be given to changing gRNA target sequences if certain gRNAs are not cutting efficiently, possibly due to the presence of gRNA-blocking motifs. The failure to obtain the desired founder can also be attributed to the microinjection operator. It is desirable that the microinjection is performed by a skilled and experienced microinjectionist.

The *in vivo* grip strength testing presents a certain level of variability and requires considerable time investment to achieve consistent reliable results. The variability may stem from several factors that include fatigue or habituation of mice to the testing procedure, behavioural changes in mice with respect to the testing environment or handling and inconsistencies in data recording by the operator. To obtain reliable and reproducible results, multiple assessments were done by the same operator, where we assayed a maximum of 3 determinations per mouse with 1-min rest intervals between each pull. The TREAT-NMD SOP DMD_M.2.2.001 elucidates the various biases that could arise irrespective of operator proficiency [15]. In one instance, one may conduct the grip strength assay in an investigator-blinded manner to mitigate the effects from this potential source of bias. In another instance, fatigue stands out as a critical factor that may introduce confounding elements into sample readings. In addressing this concern, Aartsma-Rus and colleagues recommend the inclusion of fatigue calculations across each set of readings, providing a methodological approach to mitigate potential sources of variability and ensuring a more robust evaluation of grip strength dynamics [15, 16].

Results

Generation of DMD exon deletion mouse models

We employed CRISPR-Cas9 to generate two distinct mouse models, harbouring targeted deletions of either exon-51 (ΔEx51) or exon-52 (ΔEx52) of the *Dmd* gene (Fig. 1). Firstly, we selected two gRNAs for each model that targeted the introns flanking the exon of interest, with cut site distances of 679 bp for the exon-51 deletion and 364 bp for the exon-52 deletion model to facilitate efficient founder screening via PCR (Table 2, Fig. 2A). Standard PCR genotyping with primers flanking the cut sites identified a subset of G0 (founder) pups displaying smaller amplicons, indicating the expected fragment deletions resulting from the dual CRISPR targeting. An average of 67% of G0 pups carried at

Table 1 Protocol troubleshooting guide: Common problems, causes and solution

Protocol	Step	Problem	Possible Reason	Solution
In vitro Transcription (IVT) of Guide RNAs for Cytoplasmic Microinjection	15	Unable to get founders with desired deletion	Bad quality of Cas9 mRNA	Repeat Cas9 mRNA IVT or source Cas9 mRNA from reputable source; use alternative protein form of Cas9 in microinjection
			Bad quality of one or both gRNAs	Re-visit guide RNA design and the oligos ordered. Repeat IVTs. Alternatively, change to different gRNAs
			Microinjection technical issue	Ensure that the microinjectionist possesses adequate skill and experience in the technique
Forelimb Grip Strength testing	6	Large variation in grip strength values	Technical issues by the operators	Ensure mouse handling and testing conducted by the same and experienced operator
Dystrophin Immunofluorescence	4	Unable to observe dystrophin immunofluorescence	Over-fixation	Skip fixation or perform fixation post slicing with optimised fixation reagents and duration
Western Blotting	7	Degraded Protein	Inadequate protein extraction or storage	Use fresh tissue Add protease inhibitors Keep samples on ice Avoid freeze–thaw cycles
Postmortem Tissue Processing	7	Poor tissue morphology	Improper freezing	Ensure the muscle section is not stretched when snap freezing Keep sample sizes consistent for uniform freezing Optimise the time each tissue is spent suspended in isopentane according to size

least one copy of the desired deletions. Subsequent Sanger sequencing of these PCR products confirmed the correct removal of the target exons (Fig. 2B). These founders were mated with WT mice to establish colonies.

Molecular characterisation of the generated DMD mouse models

To confirm the downstream molecular consequence of the genomic exon removal on dystrophin expression, we performed rigorous molecular analyses on muscle tissues such as quadriceps, tibialis anterior, triceps and hearts. RT-PCR across the target region demonstrated a reduction in amplicon size consistent with the absence of the deleted exons in the *Dmd* transcript (Fig. 3A, B). Sanger sequencing of the RT-PCR products corroborated these findings, confirming the expected exon deletion on RNA level and the joining of the neighbouring exons (data not shown). Notably, RT-qPCR across the terminal end of the transcript revealed a substantial reduction (85%) in the 3' end of the *Dmd* transcript, (Fig. 3C). Subsequent protein-level characterisation via Western blotting and immunohistochemistry validated the absence of dystrophin in tissues from exon-51 or exon-52 deletion mouse models (Figs. 4

and 5). These analyses confirmed the successful knockout and absence of dystrophin in the generated models.

Phenotypic characterisation of the generated DMD mouse models

It is known that mouse models lacking dystrophin, particularly those with a C57BL/6 background, do not exhibit severe phenotypes of muscle weaknesses and premature death observed in human DMD patients [8, 17]. However, dystrophin-deficient mice display measurable characteristics akin to DMD, including weaker grip strength, elevated serum CK levels, and abnormal muscle histology [8]. We systematically evaluated these parameters in our knockout mouse models and observed similar findings. Normalised grip strength assessment revealed a significant reduction in 4-week-old knockout mice compared to their WT counterparts with an average difference of twofold in grip strength and 2.5-fold increase in peak force generated across each of the three pulls, indicating compromised muscle performance due to dystrophin deficiency (Fig. 6). Additionally, serum CK levels collected from tail bleeds of the 4-week-old mice confirmed elevated levels in knockout mice of up to 16-fold compared to the WT controls (Fig. 7). Histological analysis across muscle tissue sections of our mutant models

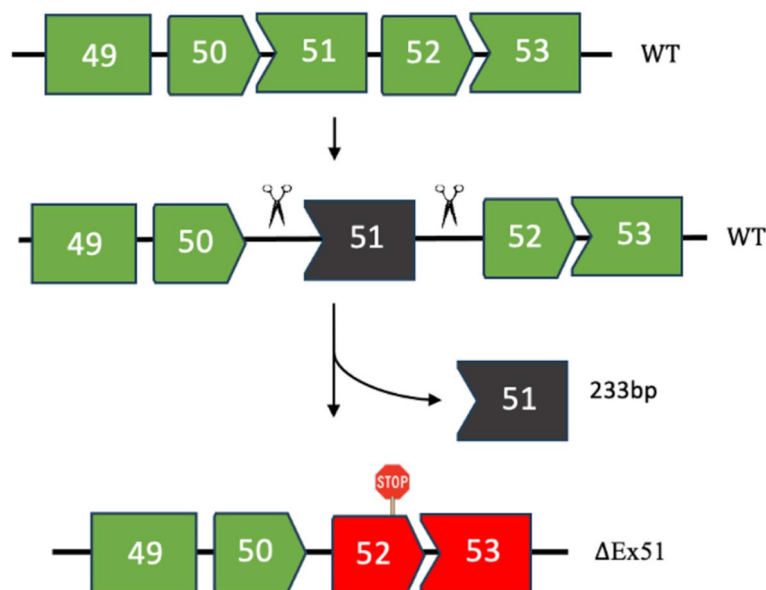


Fig. 1 CRISPR-Cas9 editing strategy for generation of mice with exon-51 deletion (Δ Ex51). Exon 52 (red) is out of frame with exon 50. The same intron-targeting strategy was applied in the context of generating an exon-52 deletion (Δ Ex52) mouse model. In the latter case, intron-51 and intron-52 were cut to result in Exon 53 being out of frame with Exon 51

Table 2 Efficiency of CRISPR-Cas9 mediated genomic editing by cytoplasm microinjection

Strain	No. of injected zygotes	No. of surviving zygotes	No. of Transferred Zygotes	No of Pups/Zygotes (%)	No of Mutant Founders/Pups (%)
<i>mDMD</i> Exon 51 KO (Δ Ex51)	136	126 (92%)	120	15 (13%)	9 (60%)
<i>mDMD</i> Exon 52 KO (Δ Ex52)	103	92 (89%)	69	26 (38%)	19 (73%)

consistently revealed dystrophic pathology characterised by centrally nucleated myofibers, fibrotic deposition, and variable myofiber size (Fig. 8). Furthermore, immunofluorescence labelling showed a lack of dystrophin in the mutant models of DMD compared with defined borders present across the sarcolemma in healthy muscle (Fig. 5). These comprehensive characterisations collectively affirm the dystrophic phenotypes evident in our knock-out models.

Discussion

In this study we generated mouse models of DMD lacking exon 51 and exon 52 of the murine dystrophin gene, representing one of the most prevalent hotspot regions of exonic deletion mutations in DMD patients. These Δ Ex51 and Δ Ex52 DMD male mice display the hallmarks of DMD, where the severity of the disease, as marked by the absence of dystrophin protein expression, muscle histology and serum CK, were comparable to other published murine models of DMD [18–20]. In a therapeutic context, correct-ing-exon 51 and exon-52 deletions through exon skipping or

reframing surrounding exons could potentially treat 8% and 12% of patients with DMD, respectively [21]. However, it is essential to recognise that these mouse models are not the most effective pre-clinical models when testing sequence-dependent therapies, as mouse and human DMD sequences are not identical. As such, mouse models harbouring targetable human DMD sequences are an attractive platform for testing genome editing strategies and other gene therapies in a more clinically relevant context [8, 22].

Interestingly, a mouse model addressing this need already exists. The first humanized DMD mouse model was developed with the full-length human DMD (hDMD) transgene integrated into chromosome 5. This model was subsequently crossed with the *mdx* strain, which lacks endogenous murine dystrophin expression [22]. Researchers have adapted these models to incorporate patient-specific mutations, such as an exon-52 deletion in hDMDTgEx52 Δ /*mdx* [23], or an exon-45 deletion in hDMDTgEx45 Δ /*mdx* and hDMDTgEx45 Δ /*mdx*D2 models [24]. However, upon closer examination, it was discovered that these hDMD models harbor a tail-to-tail

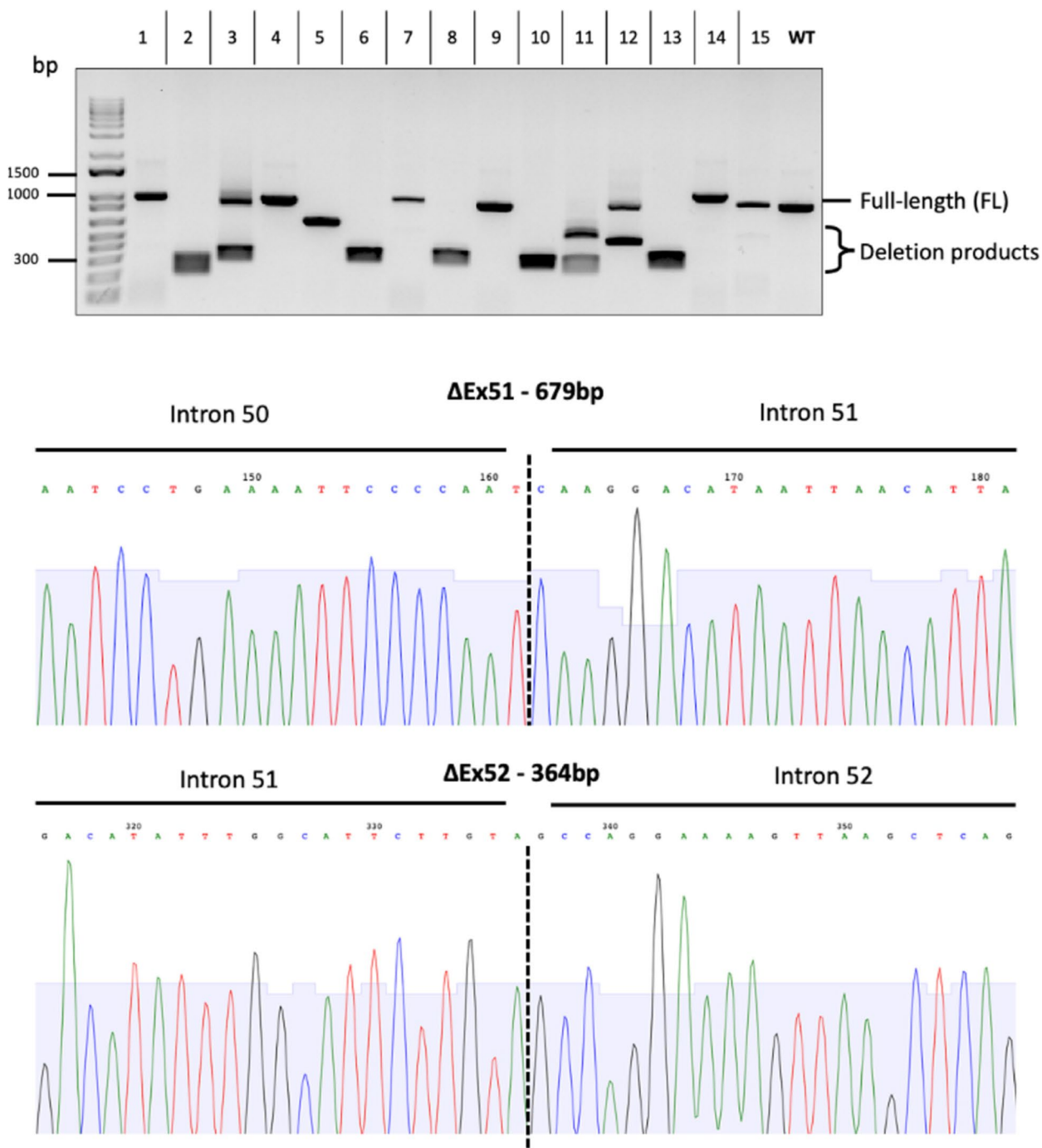


Fig. 2 Genotyping of the founders by PCR. **A** PCR primers spanned the cut sites to capture the intervening deletion resulting from the dual cut. The last sample represents the control WT band of 965 bp. **B** Sanger sequencing further confirmed the absence of exon 51 (679 bp deletion) and exon 52 (364 bp deletion) from the genomic sequence

duplication of the hDMD transgene that was likely a result of a duplication event during the original integration [23]. This dual-copy transgene arrangement does not accurately reflect the single-copy hemizygous state of the DMD gene in affected males, complicating efforts to

generate mouse models with patient-specific mutations. To overcome this issue, our lab has successfully utilised CRISPR to "de-duplicate" the hDMD transgene, creating a single-copy hDMD mouse strain that closely mimics the hemizygous state of the DMD gene in males [25]. The

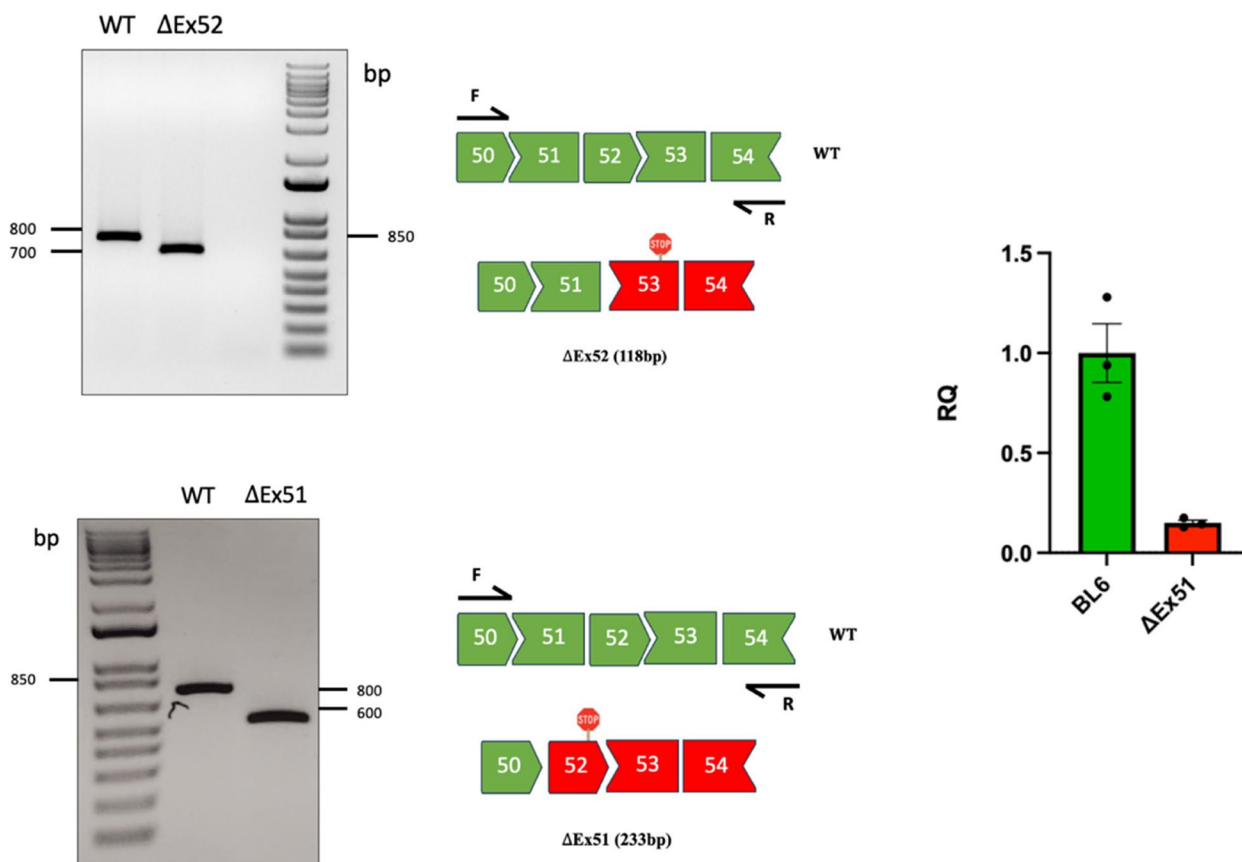


Fig. 3 RT-PCR analysis to validate the deletion of exons 51 and 52. **A, B** RT-PCR primers were in exons 50 (F) and 54 (R), and the amplicon size is 827 bp for WT mice and 594 bp for Δ Ex51 DMD mice, and 709 bp for Δ Ex52 DMD mice. RT-PCR products are schematised next to each gel image. **C** RT-qPCR analysis of transcript level differences between WT and KO, relative to the endogenous control Beta-actin. Primers span the terminal end of the DMD gene in exons 77 and 78

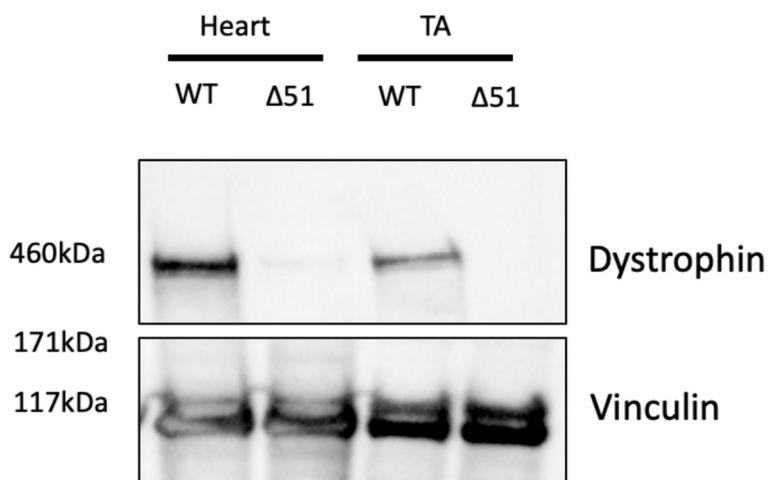


Fig. 4 Western blot from protein lysates of Δ Ex51 mice and healthy controls. 50ug of total protein was loaded per lane. There is absence of dystrophin (427 kDa) in the tibialis anterior (TA) muscle and cardiac tissues compared to controls. Vinculin was used as the loading control for normalisation

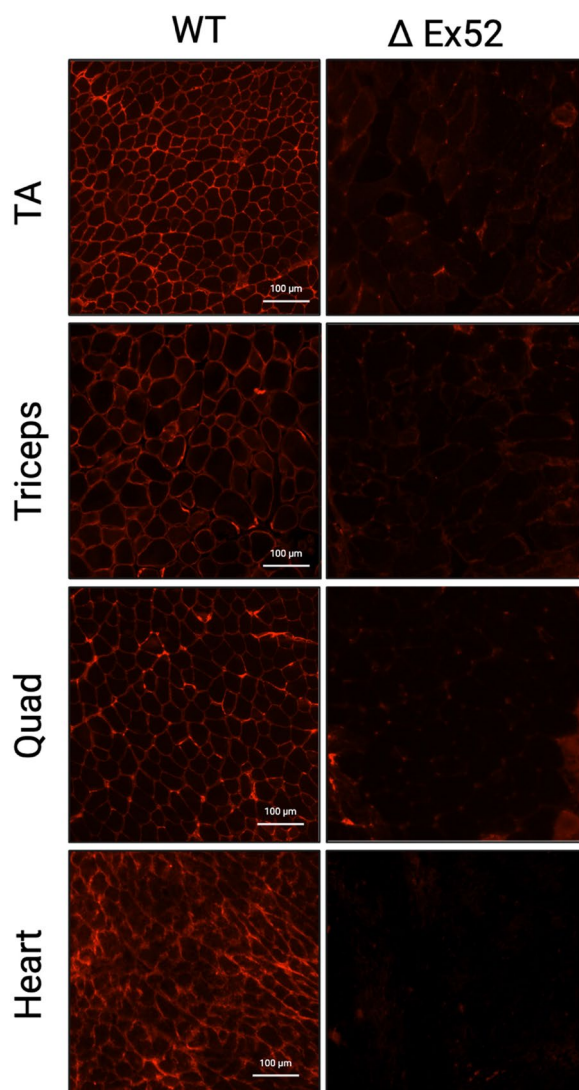


Fig. 5 Immunofluorescence indicates the absence of dystrophin in muscle tissues of Δ Ex52 DMD mice. Samples were snap-frozen in isopentane suspended within liquid nitrogen. Dystrophin is shown in red; scale bar, 100 μ m

protocols outlined in this study can be applied to generate the ideal hDMD deletion models and perform comprehensive phenotypic characterisation.

Identifying hemizygous males, who carry a single copy of the deletion, and homozygous females, who harbour the deletion on both X chromosomes, is vital for breeding purposes to maintain the DMD deletion line for further study. Discerning these specific genotypes within the founder animals enables controlled breeding to perpetuate the deletion line in subsequent generations. However, it is important to note that CRISPR-Cas9 cutting frequently induces unintended on-target large deletions that could span kilo/mega bases that will remove the primer

binding site which will be undetected by our standard PCR [26].

We observed significantly reduced transcript levels in our DMD mouse models, presumably due to Non-sense-Mediated Decay (NMD) [27]. This assay may be a valuable tool for quantifying the amount of transcript restoration when testing therapeutic guide candidates. However, a recent investigation into PTC-containing transcripts revealed that inhibiting NMD did not normalize DMD expression in an *mdx* mouse model. Instead, Spitali and colleagues (2020) hypothesised that the transcript reduction occurs through an NMD-independent epigenetically mediated mechanism through histone methylation [28].

Dystrophin typically exhibits a molecular weight of 427 kDa, corresponding to the major Dp427 muscle protein isoform. In muscle samples from individuals with DMD, the average dystrophin levels are approximately 1.3%, ranging from 0.7% to 7% of the average observed in healthy muscle [29]. Notably, dystrophin expression is a frequently employed secondary outcome measure in various clinical trials and in vivo therapeutic assessments [30]. Assessing the intensity of the dystrophin band on a blot should provide crucial information on the presence or absence of full-length dystrophin, where non-muscle dystrophin isoforms may also be expressed. Our DMD models show an absence of full-length dystrophin in both heart and TA samples. Recently, the emergence of the capillary western immunoassay has offered high-throughput analysis of dystrophin quantitation, offering greater sensitivity in detecting low-abundance proteins. This platform needs 100-fold less sample and 500-fold less antibody to detect dystrophin [29]. This automated system may provide a more accurate assessment of dystrophin expression, especially that of low-level dystrophin restoration, when assessing multiple therapeutic interventions.

Proper processing of the muscle tissue is important to study muscle biology and pathology of DMD. In alignment with what others have seen, we show that rapid freezing of freshly isolated skeletal muscle tissue using isopentane pre-cooled with liquid nitrogen and tragacanth gum was optimal for preserving tissue integrity [14]. Immersing the muscle directly into isopentane ensured rapid freezing, preventing the formation of ice crystals and ruptured cell membranes [31]. In the context of our IF results, all muscle tissues from the mutant models lack subcellular protein localisation within the sarcolemma. Haematoxylin and Eosin (H&E) staining is the gold standard approach to investigate general dystrophic pathology, giving vital information on the location of the nucleus within the fiber, muscle fiber size and fibrosis deposition [4]. In our mutant

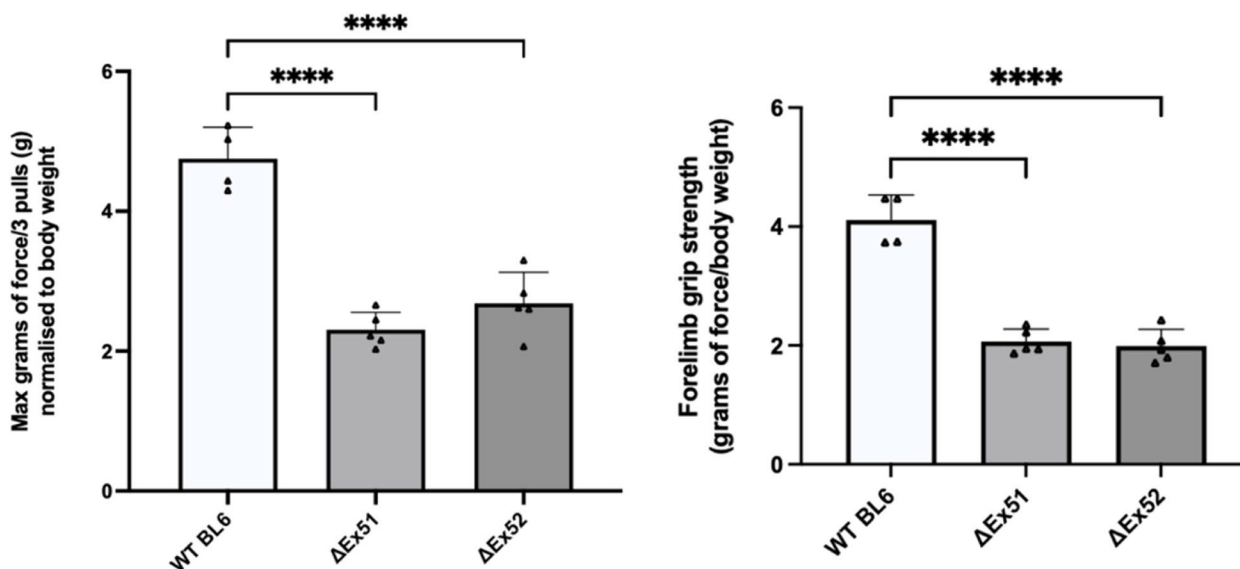


Fig. 6 Forelimb grip strength testing normalised to body weights. **A** Maximum forelimb pulls from 3 sets (4 pulls/set) each across WT, ΔEx51 and ΔEx52 mice. **B** Forelimb grip strength analysis. Data are represented as mean ± SEM. Unpaired Student’s *t*-test was performed. *****P* < 0.05 (*n* = 5)

model, these hallmarks included centrally nucleated myofibers, fibrosis deposition and variable myofiber size.

The most common biomarker in the clinical diagnosis of DMD is the serum activity levels of creatine kinase. In short, muscle contraction without dystrophin tears the sarcolemma to release creatine kinase into the bloodstream [1, 4]. Across other publications outlining other dystrophic models of DMD, we see a stark variation in CK values ranging from as low as 8 to a 40-fold difference compared to WT mice [20, 32,

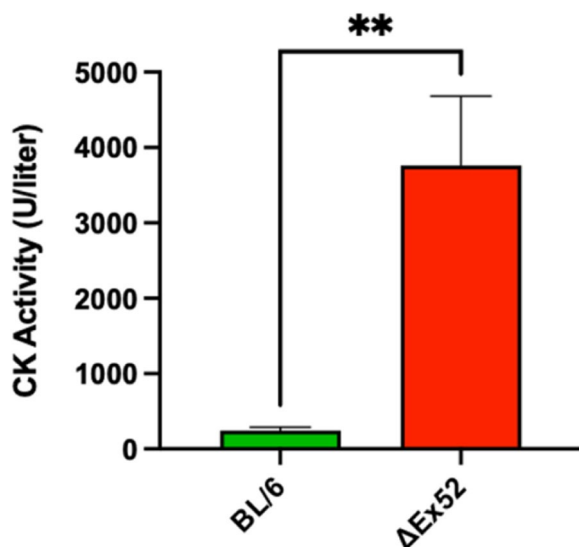


Fig. 7 Serum creatine kinase (CK), a marker of muscle damage and membrane leakage, was measured in WT (C57BL/6), ΔEx51, and ΔEx52 mice. Data represented as mean ± SEM. Unpaired Student’s *t*-test was performed. **P* < 0.005 (*n* = 5)

33]. Here we sampled an alternative route of blood collection through the lateral tail vein. The standard collection route, as recommended by TREAT-NMD has been cardiac puncture or used by labs, including submandibular vein collection. The latter method requires an anaesthesia system, but both have the limitation of being unsuitable for frequent small blood volume collection when wanting to assess CK levels at multiple time points. Our approach offers an alternative that is not limited to endpoint analysis. As evidenced in other dystrophic murine models, the analysis of serum CK levels is expected to reveal a significant elevation compared to WT mice, indicating muscle damage and membrane instability.

Much like individuals affected by DMD, the absence of dystrophin in the muscle fibres of these DMD mice renders them susceptible to exercise-induced damage, resulting in impaired muscle function compared to WT mice [4, 8]. A non-invasive functional measure such as forelimb grip strength can be used to assess this impairment and monitor the disease’s natural progression without influencing muscle pathology. Our mutant models demonstrated a noticeable reduction in the KO models compared to WT mice. This comprehensive phenotypic characterisation provides valuable insights into DMD pathology and is a pivotal tool to actively gauge the efficacy of specific treatments, including CRISPR therapy and oligonucleotide-skipping therapy. Utilising this protocol, one can actively measure the extent of therapeutic rescue, offering a dynamic assessment of treatment outcomes and advancing our understanding of potential interventions

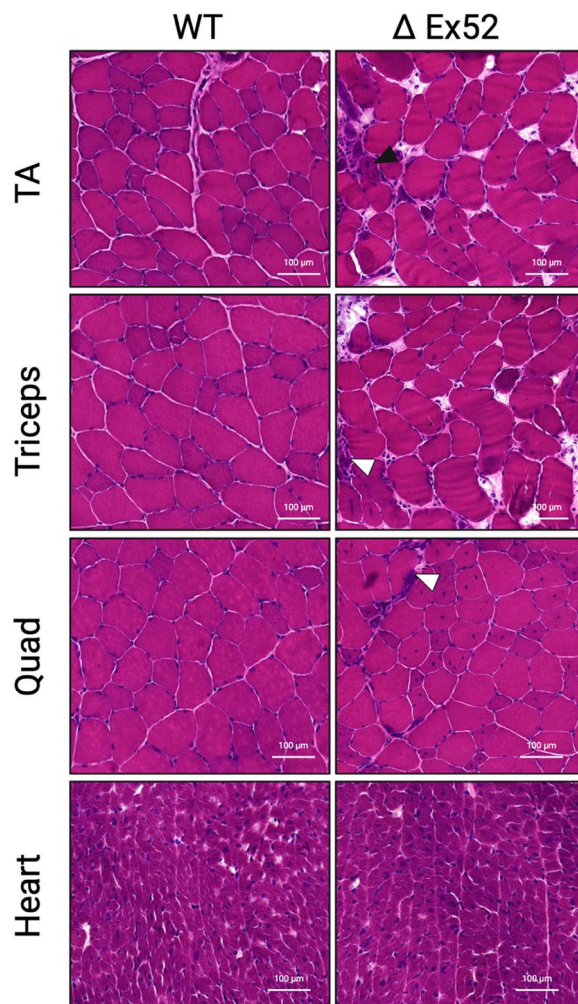


Fig. 8 Hematoxylin and eosin (H&E) stained transverse cryosections of whole tibialis anterior (TA), triceps, heart and quadriceps of WT and Δ Ex52 DMD mice. Note extensive inflammatory infiltrate, increased necrosis and fibrosis, and centralised myonuclei in DMD mice

for further development. Nevertheless, additional efforts are needed to fully characterise the DMD pathology in these models. These include a long term follow up of dystrophic mice, cardiac pathology assessment and evaluation of muscle physiology.

Off-targets are an important consideration when generating bespoke cell/animal models using CRISPR-Cas9 because the observed phenotypes from genome modifications could potentially stem from off-target effects rather than on-target modifications [34]. Therefore, it is crucial to minimise the off-target activity by performing extensive in-silico screening using reliable bioinformatic tools to identify gRNAs with limited potential off-target binding sites. In the context of generating a mutant mouse model, off-target effects at other genomic loci can

be mitigated by successive backcrossing in the breeding process to segregate away off-target mutations that may have occurred during founder generation.

Conclusion

This study presents a robust and detailed protocol for generating DMD mouse models using CRISPR-Cas9, accompanied by comprehensive molecular and phenotypic characterisation techniques. By providing step-by-step guidance on CRISPR microinjection, molecular assays, and functional tests such as forelimb grip strength and serum CK analysis, this work provides a critical framework for researchers not only developing DMD models but also those working on therapeutic interventions. These protocols serve as an invaluable resource for advancing DMD research and accelerating the development of novel treatments for the disease.

Abbreviations

DMD	Duchenne Muscular Dystrophy
CRISPR	Clustered regularly interspaced short palindromic repeats
sgRNA	Single guide RNA
DSBs	Double stranded breaks
NHEJ	Non-homologous end joining
InDels	Insertions/Deletions
IVT	In vitro-transcription
HRP	Horseshoe Peroxidase
TA	Tibialis anterior
NMD	Nonsense-mediated decay
PTC	Premature termination codon
PCR	Polymerase chain reaction
RT-PCR	Reverse transcription polymerase chain reaction
qRT-PCR	Quantitative reverse transcription polymerase chain reaction
PFA	Paraformaldehyde
H&E	Haematoxylin and Eosin
WT	wildtype
LN	Liquid Nitrogen
RFLP	Restriction fragment length polymorphism

Supplementary Information

The online version contains supplementary material available at <https://doi.org/10.1186/s44330-024-00019-y>.

Supplementary Material 1. S1 file: Step-by-step protocols, also available on protocols.io. S1 Table: Mouse Zygote injection primers and guide oligos to generate Δ Ex51 DMD mice. The T7 primer sequence is highlighted in blue. S2 Table: PCR, RT-PCR primers and SYBR Green RT-qPCR Primers. S3 Table: Antibodies used for Immunofluorescence and Western Bot analyses.

Acknowledgements

We would like to thank SAHMRI for providing the facilities to carry out leading biomedical research. We would also like to thank the South Australian Genome Editing Facility (SAGE) for assistance with generating these gene-edited models. We would like to thank Annemieke Aartsma-Rus for providing useful comments on the manuscript. BioRender was used to generate figures for this manuscript.

Authors' contributions

JA Contributed to conceptualization, contributed significantly to methodology, performed majority of investigation, formal data analysis, and data interpretation, handled all data curation, wrote first draft of the manuscript, and created all visualisations. JA also reviewed all other author manuscript suggestions and edited the final draft. YCJC contributed to methodology and

reviewed manuscript during drafting. SGP performed investigation on some aspects – including performing all microinjections. PQT and FA performed the majority of conceptualisation and methodology, project administration and supervision as well as contributed to data interpretation. Both PQT and FA performed significant revision and editing to manuscript during drafting. All authors read and approved the final manuscript.

Funding

FA. is funded by ARC DECRA scheme. Some of the experimental works were funded by the Emerging Leader Award grant awarded to FA. by The University of Adelaide, the Faculty of Health and Medical Sciences. All work involving mice was carried out with the assistance of the South Australian Genome Editing (SAGE) Facility, the University of Adelaide, and the South Australian Health and Medical Research Institute. SAGE is supported by Phenomics Australia. Phenomics Australia is supported by the Australian Government through the National Collaborative Research Infrastructure Strategy (NCRIS) program.

Data availability

Data is provided within the manuscript or supplementary information files.

Declarations

Ethics approval and consent to participate

Animal work described in this manuscript has been approved and conducted under the oversight of the Animal Ethics Committee of South Australian Health and Medical Research Institute (SAHMRI) and The University of Adelaide.

Consent for publication

Not applicable.

Competing interests

The authors declare no competing interests.

Author details

¹School of Biomedicine and Robinson Research Institute, Faculty of Health and Medical Sciences, The University of Adelaide, Adelaide, SA, Australia.

²Genome Editing Program, South Australian Health and Medical Research Institute (SAHMRI), Adelaide, SA, Australia. ³South Australian Genome Editing (SAGE), South Australian Health and Medical Research Institute (SAHMRI), Adelaide, SA, Australia.

Received: 26 March 2024 Accepted: 13 November 2024

Published online: 09 December 2024

References

- Hoffman EP, Brown RH Jr, Kunkel LM. Dystrophin: the protein product of the Duchenne muscular dystrophy locus. *Cell*. 1987;51(6):919–28. [https://doi.org/10.1016/0092-8674\(87\)90579-4](https://doi.org/10.1016/0092-8674(87)90579-4).
- Crisafulli S, Sultana J, Fontana A, Salvo F, Messina S, Trifiro G. Global epidemiology of Duchenne muscular dystrophy: an updated systematic review and meta-analysis. *Orphanet J Rare Dis*. 2020;15(1):141. <https://doi.org/10.1186/s13023-020-01430-8>.
- Bladen CL, Salgado D, Monges S, Foncuberta ME, Kekou K, Kosma K, et al. The TREAT-NMD DMD global database: analysis of more than 7,000 Duchenne muscular dystrophy mutations. *Hum Mutat*. 2015;36(4):395–402. <https://doi.org/10.1002/humu.22758>.
- Duan D, Goemans N, Takeda S, Mercuri E, Aartsma-Rus A. Duchenne muscular dystrophy. *Nat Rev Dis Primers*. 2021;7(1):13. <https://doi.org/10.1038/s41572-021-00248-3>.
- Jinek M, Chylinski K, Fonfara I, Hauer M, Doudna JA, Charpentier EA. Programmable dual-RNA-guided DNA endonuclease in adaptive bacterial immunity. *Science*. 2012;337(6096):816–21. <https://doi.org/10.1126/science.1225829>.
- Xue C, Greene EC. DNA repair pathway choices in CRISPR-Cas9-mediated genome editing. *Trends Genet*. 2021;37(7):639–56. <https://doi.org/10.1016/j.tig.2021.02.008>.
- Cong L, Ran FA, Cox D, Lin S, Barretto R, Habib N, et al. Multiplex genome engineering using CRISPR/Cas systems. *Science*. 2013;339(6121):819–23. <https://doi.org/10.1126/science.1231143>.
- Chey YCJ, Arudkumar J, Aartsma-Rus A, Adikusuma F, Thomas PQ. CRISPR applications for Duchenne muscular dystrophy: from animal models to potential therapies. *WIREs Mech Dis*. 2023;15(1):e1580. <https://doi.org/10.1002/wsbm.1580>.
- Concordet JP, Haeussler M. CRISPOR: intuitive guide selection for CRISPR/Cas9 genome editing experiments and screens. *Nucleic Acids Res*. 2018;46(W1):W242–5. <https://doi.org/10.1093/nar/gky354>.
- Ran FA, Hsu PD, Wright J, Agarwala V, Scott DA, Zhang F. Genome engineering using the CRISPR-Cas9 system. *Nat Protoc*. 2013;8(11):2281–308. <https://doi.org/10.1038/nprot.2013.143>.
- Wang H, Yang H, Shivalila CS, Dawlaty MM, Cheng AW, Zhang F, et al. One-step generation of mice carrying mutations in multiple genes by CRISPR/Cas-mediated genome engineering. *Cell*. 2013;153(4):910–8. <https://doi.org/10.1016/j.cell.2013.04.025>.
- Long C, McAnally JR, Shelton JM, Mireault AA, Bassel-Duby R, Olson EN. Prevention of muscular dystrophy in mice by CRISPR/Cas9-mediated editing of germline DNA. *Science*. 2014;345(6201):1184–8. <https://doi.org/10.1126/science.1254445>.
- Kodippili K, Vince L, Shin JH, Yue Y, Morris GE, McIntosh MA, et al. Characterization of 65 epitope-specific dystrophin monoclonal antibodies in canine and murine models of duchenne muscular dystrophy by immunostaining and western blot. *PLoS One*. 2014;9(2):e88280. <https://doi.org/10.1371/journal.pone.0088280>.
- Anwar S, Yokota T. Rapid freezing of skeletal and cardiac muscles using isopentane cooled with liquid nitrogen and tragacanth gum for histological, genetic, and protein expression studies. *Methods Mol Biol*. 2023;2587:45–53. https://doi.org/10.1007/978-1-0716-2772-3_3.
- Aartsma-Rus A, van Putten M. Assessing functional performance in the mdx mouse model. *J Vis Exp*. 2014;27(85):51303. <https://doi.org/10.3791/51303>.
- Connolly AM, Keeling RM, Mehta S, Pestronk A, Sanes JR. Three mouse models of muscular dystrophy: the natural history of strength and fatigue in dystrophin-, dystrophin/utrophin-, and laminin alpha2-deficient mice. *Neuromuscul Disord*. 2001;11(8):703–12. [https://doi.org/10.1016/S0960-8966\(01\)00232-2](https://doi.org/10.1016/S0960-8966(01)00232-2).
- Pastoret C, Sebille A. mdx mice show progressive weakness and muscle deterioration with age. *J Neurol Sci*. 1995;129(2):97–105. [https://doi.org/10.1016/0022-510x\(94\)00276-t](https://doi.org/10.1016/0022-510x(94)00276-t).
- van Putten M, de Winter C, van Roon-Mom W, van Ommen GJ, 't Hoen PA, Aartsma-Rus AA. 3 months mild functional test regime does not affect disease parameters in young mdx mice. *Neuromuscul Disord*. 2010;20(4):273–80. <https://doi.org/10.1016/j.nmd.2010.02.004>.
- Chemello F, Wang Z, Li H, McAnally JR, Liu N, Bassel-Duby R, Olson EN. Degenerative and regenerative pathways underlying Duchenne muscular dystrophy revealed by single-nucleus RNA sequencing. *Proc Natl Acad Sci USA*. 2020;117(47):29691–701. <https://doi.org/10.1073/pnas.2018391117>.
- Min YL, Chemello F, Li H, Rodriguez-Caycedo C, Sanchez-Ortiz E, Mireault AA, et al. Correction of three prominent mutations in mouse and human models of Duchenne muscular dystrophy by single-cut genome editing. *Mol Ther: J Am Soc Gene Ther*. 2020;28(9):2044–55. <https://doi.org/10.1016/j.jymthe.2020.05.024>.
- Aartsma-Rus A, Fokkema I, Verschuuren J, Ginjaar I, van Deutekom J, van Ommen G, et al. Theoretic applicability of antisense-mediated exon skipping for Duchenne muscular dystrophy mutations. *Hum Mutat*. 2009;30(3):293–9. <https://doi.org/10.1002/humu.20918>.
- 't Hoen PA, de Meijer EJ, Boer JM, Vossen RH, Turk R, Maatman RG, et al. Generation and characterization of transgenic mice with the full-length human DMD gene. *J Biol Chem*. 2008;283(9):5899–907. <https://doi.org/10.1074/jbc.M709410200>.
- Yavas A, Weij R, van Putten M, Kourkouta E, Beekman C, Puolivali J, et al. Detailed genetic and functional analysis of the hDMDdel52/mdx mouse model. *PLoS One*. 2020;15(12):e0244215. <https://doi.org/10.1371/journal.pone.0244215>.
- Young CS, Mokhonova E, Quinonez M, Pyle AD, Spencer MJ. Creation of a novel humanized dystrophic mouse model of Duchenne muscular dystrophy and application of a CRISPR/Cas9 gene editing therapy. *J Neuromuscul Dis*. 2017;4(2):139–45. <https://doi.org/10.3233/JND-170218>.

25. Chey YC, Corbett M, Arudkumar J, Piltz S, Thomas PQ, Adikusuma F. CRISPR-mediated megabase-scale transgene de-duplication to generate a functional single-copy full-length humanized DMD mouse model. *BMC Biol.* 2024. <https://doi.org/10.1101/2024.03.25.586713>.
26. Adikusuma F, Piltz S, Corbett MA, Turvey M, McColl SR, Helbig KJ, et al. Large deletions induced by Cas9 cleavage. *Nature.* 2018;560(7717):E8–9. <https://doi.org/10.1038/s41586-018-0380-z>.
27. Brogna S, Wen J. Nonsense-mediated mRNA decay (NMD) mechanisms. *Nat Struct Mol Biol.* 2009;16(2):107–13. <https://doi.org/10.1038/nsmb.1550>.
28. García-Rodríguez R, Hiller M, Jiménez-Gracia L, van der Pal Z, Balog J, Adamzek K, et al. Premature termination codons in the *DMD* gene cause reduced local mRNA synthesis. *Proc Natl Acad Sci USA.* 2020;117(28):16456–64. <https://doi.org/10.1073/pnas.1910456117>.
29. Beekman C, Janson AA, Baghat A, van Deutekom JC, Datson NA. Use of capillary Western immunoassay (Wes) for quantification of dystrophin levels in skeletal muscle of healthy controls and individuals with Becker and Duchenne muscular dystrophy. *PLoS One.* 2018;13(4): e0195850. <https://doi.org/10.1371/journal.pone.0195850>.
30. Anthony K, Arechavala-Gomez V, Taylor LE, Vulin A, Kaminoh Y, Torelli S, et al. Dystrophin quantification: Biological and translational research implications. *Neurology.* 2014;83(22):2062–9. <https://doi.org/10.1212/WNL.0000000000001025>.
31. Kumar A, Accorsi A, Rhee Y, Girgenrath M. Do's and don'ts in the preparation of muscle cryosections for histological analysis. *J Vis Exp : JoVE.* 2015;99:e52793. <https://doi.org/10.3791/52793>.
32. Karri DR, Zhang Y, Chemello F, Min YL, Huang J, Kim J, et al. Long-term maintenance of dystrophin expression and resistance to injury of skeletal muscle in gene edited DMD mice. *Mol Ther Nucleic Acids.* 2022;28:154–67. <https://doi.org/10.1016/j.omtn.2022.03.004>.
33. Zhang Y, Nishiyama T, Li H, Huang J, Atmanli A, Sanchez-Ortiz E, et al. A consolidated AAV system for single-cut CRISPR correction of a common Duchenne muscular dystrophy mutation. *Mol Ther Methods Clin Dev.* 2021;22:122–32. <https://doi.org/10.1016/j.omtm.2021.05.014>.
34. Fu Y, Foden JA, Khayter C, Maeder ML, Reyon D, Joung JK, et al. High-frequency off-target mutagenesis induced by CRISPR-Cas nucleases in human cells. *Nat Biotechnol.* 2013;31(9):822–6. <https://doi.org/10.1038/nbt.2623>.

Publisher's Note

Springer Nature remains neutral with regard to jurisdictional claims in published maps and institutional affiliations.